

Extracellular Recordings of Synaptic Plasticity and Network Oscillations in Hippocampal Slices

Gaga Kochlamazashvili, Oleg Senkov, and Alexander Dityatev

Abstract

Activity-dependent strengthening and weakening of synaptic weights, manifested as long-term potentiation (LTP) and depression (LTD), are two major mechanisms that are thought to be involved in creating memory traces in the brain. Oscillations of neuronal activity, especially in the θ (4–12 Hz), γ (30–100 Hz), and “ripple” (130–200 Hz) frequency bands, are also fundamental phenomena that are believed to contribute to learning and memory. However, the interplay between oscillations and plasticity is still not understood. These brain phenomena are rarely considered together when synaptic plasticity is studied. In this chapter, we summarize the existing knowledge in the field, describe protocols that can be used to induce LTP in seven major excitatory synaptic pathways in hippocampal slices, and introduce a procedure to investigate synaptic plasticity and induce high-frequency oscillations under one experimental paradigm.

Key words: LTP, LTD, Synaptic plasticity, Learning, Theta, Gamma, Oscillation

1. Introduction

The phenomenon of LTP of synaptic transmission has been first discovered in vivo in anesthetized rabbits. In 1966, Terje Lomo first registered the potentiation of field excitatory postsynaptic potentials (fEPSPs) in granular cells in the hippocampal dentate gyrus (DG) after the application of repetitive trains of stimuli to the main input of the DG—perforant path (PP). Then, with Tim Bliss, he further investigated this phenomenon in the beginning of 1970s (1). Since then, research regarding LTP, as a leading cellular and network model of learning and memory, made a gigantic leap in deciphering the molecular and synaptic mechanisms of the encoding/decoding of memory traces (2). In vivo studies of LTP and the opposite phenomenon (i.e., LTD) widely paralleled the majority of in vitro experiments and brought ample new information about experience- and activity-dependent synaptic plasticity in freely behaving animals. Experiments using anesthetized animals (especially rats) also extended our knowledge about how the brain perceives, operates and learns in paradigms

34 such as associative eyelid conditioning, stimulus discrimination in
35 the barrel cortex, ocular dominance and auditory plasticity (3).
36 During 40 years of LTP research, synaptic plasticity was found in
37 nearly all input/output extrahippocampal, cortical, thalamic, and
38 cerebellar excitatory synapses, including the amygdala (4–6), cere-
39 bellum (7, 8), and the prefrontal (9), entorhinal (10), visual (11),
40 and somatosensory (12) cortices.

41 The phenomenon of brain oscillations is also well and long
42 known in neuroscience and clinical studies since the discovery in
43 the late twentieth of the last century Berger's electroencephalo-
44 graphic (EEG) waves registered from the surface of a human scalp
45 (13, 14). From that time, brain oscillations recorded with the use
46 of different invasive and noninvasive techniques and paradigms
47 had been widely explored, and a strong link between brain waves
48 and perception, cognition, learning and memory in humans and
49 animals has been established (15). However, little is known about
50 how these two ultimate brain phenomena interact during encod-
51 ing, decoding, storage and retrieval of memory traces in normal
52 and pathological conditions. The major goal of this chapter is to
53 overview the studies, in which these two phenomena were
54 addressed together and to outline one of options how to method-
55 ologically merge in one experimental scope investigation of syn-
56 aptic plasticity and network oscillations at different synapses of
57 mouse hippocampal formation in vitro.

1.1. Oscillations In Vivo

58 The mammalian brain constantly generates a variety of oscillations
59 that differ in amplitude and frequency (from 0.05 to 500 Hz),
60 depending on the brain state and ongoing behavior (16–18).
61 Brain oscillations in the θ (4–12 Hz) and γ (30–100 Hz)
62 frequency ranges are most prominent in the areas with the highest
63 cognitive and computational loads (e.g., in the hippocampus and
64 cortex), suggesting their potential roles in perception, learning
65 and memory. The θ rhythm can be readily observed in all layers
66 and regions of the excitatory trisynaptic circuitry of the hippocam-
67 pus, but it is most regular in frequency and largest in amplitude in
68 the *stratum lacunosum-moleculare* (*str. lac-mol.*) of the CA1
69 region. A θ rhythm that is smaller (by factor of 5–10) in power
70 can also be recorded in vivo in many cortical and subcortical
71 structures (e.g., the subicular, entorhinal, perirhinal, cingulate,
72 and prefrontal cortices and the amygdala). In rodents, there are
73 two types of hippocampal θ rhythms: high θ (8–12 Hz), which
74 depends on ongoing motor activity and the engagement of
75 the brain while exploring the environment, and low cholinergic-
76 dependent θ (5–8 Hz), which is triggered by medial septum
77 activation and can be fully erased by atropine or scopolamine.
78 The highest-amplitude θ rhythm occurs during exploratory behav-
79 ior and REM sleep. The firing of many cells in the hippocampus,

especially principal pyramidal neurons, is phase-locked to the θ rhythm (19), which means that they mostly fire in a certain phase of the rhythm. In particular, so-called “place cells”, which encode space and create a navigational map for the animal are locked into the θ rhythm. The phase of firing of place cells relative to the θ rhythm changes systematically when the animal approaches a specific location (20, 21).

An important role for the hippocampal θ rhythm in synaptic plasticity is suggested by several observations: (1) The most prominent θ rhythm occurs while exploring a new environment and generating a spatial map of this environment. (2) Spatial learning is impaired when the θ rhythm is disrupted (e.g., via a lesion in the medial septal nucleus) (22). (3) The excitation of hippocampal principal cells is phase-coupled to the θ waves. (4) Trains of stimuli that are delivered to mimic the θ pattern induce LTP more readily than stimulation at other frequencies.

Several recent studies strengthen a link between oscillations and plasticity. HFS (200 Hz, 15 stimuli, 10 bursts, 10-s interburst interval, with an intensity of 40% from the maximal response) of the medial PP induces an increase in the θ power and facilitates γ oscillations in the DG. These changes occurred in rats that could develop LTP or short-term potentiation (STP) but not in a group of animals that failed to show potentiation. The increased γ and θ rhythms in the DG of freely moving rats can persist up to 24 h after tetanization (23, 24). The delivery of HFS (3 bursts, 5 pulses of 400 Hz in each burst) to the CA3–CA1 synapses of freely moving rats was also effective for inducing long-lasting (1 h) LTP (if tetanization was applied at the θ peaks) or LTD (if it was applied at the θ troughs). These experiments clearly demonstrated that LTD can be induced in the hippocampus by a physiological pattern of stimulation and without using artificial long trains of low-frequency stimulation (LFS) (25).

The same effect was observed in urethane-anesthetized rats when the θ rhythm was generated by sensory stimulation (26). Sensory stimulation can induce θ -like oscillations in anesthetized animals. For instance, a tail-pinch can be used to trigger the θ rhythm. The application of brief bursts of stimuli (5 pulses, 200 Hz) during different phases of a tail-pinch-evoked θ rhythm can mimic naturally occurring neuronal activity much more closely than either standard HFS or LFS. A single burst of 5 pulses at 200 Hz delivered to a θ peak can evoke 20% potentiation of CA1 synapses that is stable for 60 min. Notably, LTP can be gradually increased up to 50–60% from baseline if three bursts are applied. Using a similar paradigm, LTP can be evoked in other synapses (e.g., PP-DG granule cell layer synapses), if the tetanus is delivered to a positive peak of θ in urethane-anesthetized rats (27, 28).

126 Such bidirectional synaptic modifications induced by the pairing of
127 θ waves and HFS can persist up to 48 h in freely moving rats (29).

128 In another interesting work, the firing patterns of CA1 place
129 cells were analyzed during REM sleep (30), which is known to be
130 vital for memory consolidation. When rats experienced a familiar
131 environment, the place cells tended to fire in troughs of θ waves
132 during the subsequent REM sleep, which is consistent with the
133 induction of LTD. However, after the rats were exposed to a novel
134 maze, place cell firing shifted to the peaks of the θ oscillations,
135 which is consistent with the induction of LTP. Such a transition in
136 the θ phase from a novel to an explored context is built up
137 gradually over several days, as rats became familiar with the
138 novel environment. It was concluded that, perhaps, the remote
139 memory traces that are encoded in a familiar place are erased
140 during subsequent REM sleep, whereas the traces of recent
141 experiences that are acquired while facing a novel environment
142 are strengthened.

1.2. Oscillations In Vitro

143 Oscillating network activity can also be induced and manipulated
144 pharmacologically in brain slices. For example, robust θ oscillations
145 can be induced by perfusion with cholinergic agonists, such
146 as carbachol. A series of studies has shown that only one burst
147 (4 pulses, 100 Hz) of Schaffer collateral/commissural pathway
148 stimulation administered during the peak of carbachol-induced
149 oscillations resulted in the LTP of CA1 fEPSPs, and one burst
150 presented at the trough depotentiated these synapses (31, 32).

151 Cholinergic activation can induce higher-frequency oscillations
152 in addition to the θ rhythm. For example, temporally stable
153 (up to 1 h) and very coherent network activity at γ frequencies
154 (about 30–35 Hz) can be induced at the CA3 *stratum pyramidale*
155 and *radiatum* (*str. pyr.*, *str. rad.*) by the bath application of carba-
156 chol to rat hippocampal slices (33). The γ oscillations in these two
157 layers are phase-reversed and alternate periodically, similar to those
158 reported in vivo (34). During γ oscillations, pyramidal cells fire at
159 the negative peak of the oscillations, which is followed by the
160 discharge of interneurons that form a recurrent loop with pyrami-
161 dal cells. This gives rise to the precise timing of firing of pyramidal
162 cell assemblies at γ frequencies. Fast-spiking perisomatic inhibitory
163 interneurons are the most active cell type during γ oscillations that
164 have a strong phase coupling to the γ rhythm, whereas the majority
165 of interneurons that target the dendritic regions of pyramidal cells
166 do not exhibit significant phase-coupled firing.

167 In the CA1 and DG regions of the hippocampus, large-amplitude
168 β (14–30 Hz) and γ oscillations can be elicited by the application of
169 glutamate or by the tetanic stimulation of afferents (35, 36). These
170 and other studies indicate that the role of oscillations in synaptic
171 plasticity in vitro can be addressed by several different paradigms.
172 First, a pharmacological approach can be utilized; synchronous

oscillations can be induced via application of different activators of neuronal activity, such as agonists of cholinergic muscarinic, glutamate metabotropic or kainate receptors, or via changing the ionic composition of the extracellular solution (e.g., by decreasing Ca^{2+} and increasing K^+). Second, electrical stimulation (tetanization) of presynaptic terminals with different stimulation protocols can be used to evoke short and locked to stimulus-onset oscillations. Such tetanization can be applied to different neuronal pathways within one brain structure or even to distinct structures (e.g., hippocampus and amygdala). Thus, the role of long-range synchronization in synaptic plasticity can be studied. To facilitate the induction of oscillations, a combination of the aforementioned methods can be used.

It is well known that in contrast to *in vivo* recordings, spontaneous oscillations are rarely detected in hippocampal slices under basal conditions. However, prominent hippocampal atropine-resistant θ rhythm (3–10 Hz) is readily detectable in the whole hippocampus *in vitro* recording (37), where majority of its intrinsic pathways are preserved. In this elegant study, authors demonstrated existence of multiple self-sustained cholinergic-, medial septum-, and CA3-independent theta oscillators located along the longitudinal axis of CA1 area of the hippocampus. Their θ oscillations could be blocked by antagonists of GABA_A or AMPA/kainate receptors, but not with muscarinic acetylcholine receptor antagonists. By contrast, carbachol-induced θ activity in slices does not require involvement of inhibition through GABA_A receptors, and CA3 neurons take part in θ generation. Thus, multiple network and molecular mechanisms are responsible for generating θ oscillations in slice and whole hippocampus preparations.

1.3. Synaptic Plasticity and Oscillations

Although the majority of studies in the synaptic plasticity field were conducted using an artificial forced synchronized activation of afferents, a few available publications suggest an important link between plasticity and naturally occurring or induced spontaneous oscillations. Oscillations at the θ and γ frequencies may provide temporal windows in which distinct neuronal populations can fire synchronously, allowing temporally functional assemblies to be formed to encode a common feature of the environment or a task (38). Such temporal segregation via oscillations, in turn, favors synaptic plasticity, perception, learning, and memory. A recent study conducted by Moser's group strengthens this idea of routing flow of information by oscillations (39) and supporting the view that two different frequencies of γ oscillations, slow (25–50 Hz) and fast (65–140 Hz), are responsible for different functions in the hippocampus. Fast γ synchronizes CA1 and medial entorhinal cortex during encoding spatial information, whereas slow CA1 γ is locked to CA3 and supports retrieval of stored memory. These two γ oscillations predominantly occur at

220 different phases of θ cycle and mostly on different θ cycles in CA1.
221 Moreover, fast γ power is maximal at the θ phase when place cells
222 are most likely to fire, and slow γ occurred primarily at the θ phase
223 when CA1 place cells fire with low probability, due to CA3 feed-
224 forward inhibition of CA1 area. These results provide a mecha-
225 nism for temporal segregation of information transmitted to CA1
226 from the entorhinal cortex and CA3.

227 Synaptic weights can be modulated by the θ rhythm and
228 higher-frequency oscillations by the “peak-trough” rule. For
229 example, in the rat visual cortex, the synapses of the pyramidal
230 cells in layer II exhibited LTP when the EPSPs coincided with the
231 peaks of the oscillations in the β and γ frequency bands (20 and
232 40 Hz, respectively), but they exhibited LTD if the EPSPs coin-
233 cided with the troughs. These results suggest that, when neuronal
234 networks engage in high-frequency oscillations, synaptic plasticity
235 remains exquisitely sensitive to the timing of the discharges. The
236 precise synchronization of discharges serves as a signature of relat-
237 edness during distributed processing. Thus, the temporal relations
238 among the discharges of interconnected neurons are important
239 variables in synaptic plasticity. Synapses undergo LTP when the
240 EPSP precedes the postsynaptic spike by within a few tens of
241 milliseconds, and they undergo LTD when the EPSP follows the
242 spike, exhibiting so-called “spike time-dependent plasticity” (40).

1.4. Future Directions for Research

243 In following methodological sections, we first describe protocols
244 for the induction of LTP by TBS or HFS in several subtypes of
245 hippocampal synapses, which have distinct mechanisms of synaptic
246 plasticity. For example, LTP in CA3-CA1 synapses depends on
247 signaling via NMDA-Rs, whereas LTP is NMDA-R independent
248 in mossy fiber-CA3 synapses. To understand the role of a particu-
249 lar molecule in synaptic plasticity, it is tempting to investigate how
250 manipulating the expression of that molecule may affect plasticity
251 in distinct types of synapses (41) or to use various paradigms for
252 the induction of synaptic plasticity, which involve distinct induc-
253 tion mechanisms (42). Owing to specific roles played by different
254 hippocampal synapses in cognitive functions (3), it is attractive to
255 analyze all of the major excitatory synaptic connections in the
256 hippocampal circuitry in combination with a behavioral analysis
257 of cognition. This approach can help to merge synaptic and cog-
258 nitive functions.

259 Second, we introduce an HFS protocol (20 pulses at 100 Hz
260 at a high stimulation intensity) that induces high-frequency oscil-
261 lations in the pyramidal layer, which are followed by the LTP of
262 CA3-CA1 synapses. This protocol mimics a commonly found
263 situation in which a short sensory stimulus is followed by induced
264 oscillations. Importantly, when 20 pulses are applied at 100 Hz
265 but with a stimulation intensity that does not induce oscillations,
266 no LTP is induced. Furthermore, mice that are deficient in anion

exchanger 3, exhibit more prominent oscillations and increased LTP following these oscillations, as compared to wild-types (Kochlamazashvili and Dityatev, unpublished data). These data suggest that a pairing of synaptic activity with neuronal oscillations, even with the considerable delay of a 100 ms, could contribute to the enforcement of the stimulated synapses. Possible mechanisms may involve the back-propagation of the spikes that are generated during these oscillations to the synapses that are located on dendrites of pyramidal cells. These spikes can activate postsynaptic voltage-gated L-type Ca^{2+} channels or relieve the Mg^{2+} block of NMDA-Rs bound to glutamate that was released during HFS. Further work is needed to elucidate these mechanisms. Furthermore, by adding another electrode to stimulate independent afferent pathways during induced oscillations, this paradigm could be extended to investigate the mechanisms of oscillation- and spike time-dependent plasticity.

2. Materials

2.1. Materials for Slice Preparation

1. A vessel connected by tubing to a regulated CO_2 supply (for mouse sedation).
2. A vibratome (e.g., VT 1200S, Leica).
3. Razor blades (a new blade is used for each slice preparation).
4. A mounted-line gas mixture (95% O_2 /5% CO_2) with a regulator.
5. A diffuser (aquarium air stone, with tubing of an appropriate diameter to connect the regulator and the air stone).
6. Agar blocks and solution (agarose from Sigma Aldrich).
7. A water bath (e.g., TW 12, Julabo).
8. A plastic chamber for incubating the brain slices.
9. Rapid glue (Vetbond).
10. A small weighing spatula, scalpel, forceps, large scissors, small sharp-nosed dissecting scissors and a soft small paintbrush for transferring the slices (FST).

2.2. Materials for fEPSP Recording in Hippocampal Slices

1. Three micromanipulators (Scientifica).
2. An upright microscope (BX61WI Olympus).
3. An amplifier (EPC10 HEKA).
4. A stimulus isolator unit (A360 World Precision Instruments).
5. A workstation (Dell).
6. A recording chamber (Warner Instruments).

- 304 7. A perfusion system, consisting of a 500-ml plastic container
305 with an aquarium stone for babbling the ACSF and polyeth-
306 ylene tubing for circulating the ACSF under the control of a
307 peristaltic pump (Gilson).
- 308 8. A mounting-line heater to control the temperature of the
309 ACSF (Ala Scientific Instruments).
- 310 9. A homemade platform for the slices, consisting of a nylon
311 mesh glued onto a metal half-circle to perfuse the slices with
312 ACSF from both sides more effectively.
- 313 10. Small pieces of nylon mesh (7×10 mm, Millipore) with a
314 hole (2 mm in diameter) in the middle.
- 315 11. Two small metal loads to fix the mesh onto the recording
316 platform.
- 317 12. Glass pipettes for extracellular recordings (Hilgenberg).
- 318 13. A glass microelectrode puller (Sutter Instruments).

3. Methods

319

320 Here, we describe the methods that are used for the extracellular
321 recordings of synaptic plasticity and oscillations in vitro. These
322 include the preparation of the hippocampal slices, the recording
323 and analysis of field excitatory postsynaptic potentials (fEPSPs),
324 the induction of short- and long-term synaptic plasticity in differ-
325 ent synaptic connections in the hippocampus and the induction
326 of oscillatory activity in the CA1 region using a short tetanic
327 stimulation.

328 Importantly, the hippocampal slices remain viable for several
329 hours, and stable recordings can be carried out at visually controlled
330 recording sites. Bath application of the determined concentrations
331 of the pharmacological agents, which can be easily washed in and
332 out, is an exceptionally useful advantage of using in vitro methods
333 for pharmacological studies. The drugs can also be applied using
334 visually guided micropipettes to discrete neuronal regions that con-
335 sist of well-defined hippocampal layers and subareas. In such
336 preparations, the cell bodies of the pyramidal neurons lie in a single
337 densely packed layer that is clearly apparent. This layer is divided into
338 several distinct regions, including CA1, CA2, and CA3. The den-
339 drites of the pyramidal cells in the CA1 region form a thick band
340 (str. rad.), where they receive synapses from the axons of the pyra-
341 midal cells in the CA3 region. The CA3–CA1 synapse is the most
342 widely studied synapse in the hippocampus due to its simple identi-
343 fication. Therefore, here we concentrate on protocols to study this
344 synapse and only briefly describe the protocols for recording LTP in
345 the other major excitatory hippocampal synapses.

3.1. Methods for Slice Preparation

Hippocampal slices for synaptic plasticity experiments can be prepared from juvenile, adult or old mice. We could reliably record LTP from 10-day- to 2-year-old mice (see Notes, Sect. 1) A mouse is placed in a closed transparent plastic vessel, into which CO₂ is slowly released via regulated mounted-line tubing until the mouse is sedated. Next, the mouse is quickly decapitated using large scissors, and the head is placed in a Petri dish filled with ice-cold oxygenated (with a mixture of 95% O₂ and 5% CO₂) dissection artificial cerebrospinal fluid (dACSF), containing the following substances (in mM): sucrose 250, NaHCO₃ 24, glucose 25, KCl 2.5, NaH₂PO₄ 1.25, CaCl₂ 2, MgSO₄ 1.5, pH 7.35–7.4. The mouse head is fixed using forceps inserted into the eye-sockets; the skin is then cut from the skull and removed using small sharp-nose scissors. The bones are cut up to the parietal bones using small scissors, with one sharp end inserted underneath the skull from the spinal cord side. With small bent forceps, the occipital, interparietal, parietal, and frontal bones are broken and removed from the brain surface. The brain is then quickly removed using a small spatula and placed into another Petri dish with the same ice-cold oxygenated dACSF. It is important to minimize time that is required for this step (to 1–1.5 min) to avoid the ischemic death of the brain tissue. The cerebellum is then dissected away, and the brain cut along the midline into two equal hemispheres using a sharp scalpel. One hemisphere is immediately glued (using a rapid glue) onto the object-mounting platform with a cutting surface (for recordings in the CA1 field) adjacent to a 1-cm³ cubic 20%-agar block, which is glued to the mounting platform prior to brain dissection and is used as a support for the brain tissue during slicing. The brain hemisphere is covered with 10% warm (kept in a water bath) liquid agar (to embed the brain tissue and fill the gap between it and the agar block) and placed in a vibratome buffer tray filled with ice-cold, continuously oxygenated dACSF. The other hemisphere is placed into the same buffer tray to be sliced later. For CA3 recordings, the ventral surface of each hemisphere is cut at an angle of 20°, and this surface is glued to the platform (43). For recordings in other synapses, either sagittal or horizontal slicing is used, as indicated below. The cerebral hemisphere that is attached to the platform is then cut into slices using the vibrotome (see Notes, Sect. 2). The agar, which is used to cover the brain tissue, protects the brain from deformation during cutting and from the unwanted release of the brain hemisphere from the platform. The slices are separated from their agar surroundings using a small soft paintbrush and transferred to the slice incubation chamber using a small spatula. The slices are maintained in ACSF (120 mM NaCl instead of 250 mM sucrose in dACSF) for 1.5–2 h before their use in the incubation chamber (see Notes, Sect. 3). The ACSF should be previously bubbled for at least 30 min at room temperature before slice transfer.

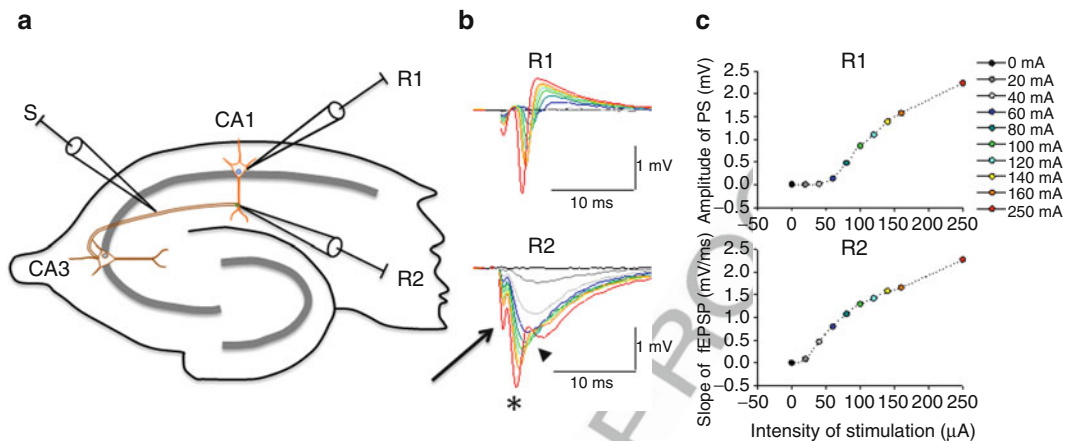


Fig. 1. Design of extracellular recordings in the CA3–CA1 connections. (a) Schematic illustration of a hippocampal slice and the positioning of electrodes for the recording of fEPSP and PSs in the CA1 region. S, stimulating electrode; R1, recording electrode in the *stratum pyramidale*; R2, recording electrode in the *stratum radiatum*. (b) Traces representing responses in R1 and R2 evoked by stimulation with increasing stimulus strengths (from 0 to 160 μA with 20- μA steps and a stimulation intensity of 250 μA). The *upper panel* shows the appearance of PSs with increasing stimulation intensities at electrode R1. The *lower panel* shows recordings of the fEPSPs (a peak indicated by *asterisk*) from *stratum radiatum*. The early component preceding fEPSP is a presynaptic volley (indicated by *arrow*). At 160 μA (but not at lower intensities), the “supramaximal” fEPSP is evoked in the *stratum radiatum*, which is superimposed with a PS (indicated by *arrowhead*). A single supramaximal stimulation at 250 μA was given to show the responses at the stimulation strength that was most effective for inducing oscillations (see Fig. 4). At 250 μA , both the fEPSP and PS are clearly distinguishable. (c) Stimulus intensity-response curves for the PS amplitude (*upper panel*) and the slope of the fEPSPs (*lower curve*). The color code represents measurements at different stimulation intensities.

3.2. Methods for fEPSP Recording In Vitro

For fEPSP recording in hippocampal slices, we used the procedures described below. A hippocampal slice is transferred into the recording chamber (see Notes, Sect. 4) using a paintbrush and spatula. Good-quality slices can be recognized under a light microscope at 4 \times magnification by clearly visible pyramidal and granule cell layers (which are lighter than the surrounding tissue). The recording and stimulating glass pipettes are prepared in advance with previously determined shapes and filled with ACSF. The electrodes for the extracellular recording of the fEPSPs usually have resistances of 2 M Ω , whereas the stimulation electrode has a resistance less than 1 M Ω . We used one stimulation electrode (S) and two recording electrodes (R1 and R2, Fig. 1). R1 is used for the recording of population spikes (PSs) in the *str. pyr.*, and R2 is used for recording fEPSPs in the *str. rad.* (Fig. 1). All three electrodes are gently placed onto the surface of the slice in a configuration such that the recording electrodes are about 200–250 μm apart from the stimulating electrode, which is located in the *str. rad.* (Fig. 1a). It is important to first place the stimulating electrode slightly away from the pyramidal cell layer and then slowly deepen it within the tissue. Recording electrode R2 is placed in the *str. rad.* at about the same depth and distance from the pyramidal cell layer (Fig. 1a). Recording electrode R1 is located in the pyramidal cell layer at about the same distance

394
395
396
397
398
399
400
401
402
403
404
405
406
407
408
409
410
411
412
413
414
415

from the stimulating electrode (Fig. 1a). Stimulation (50–70 μ A, 416
0.2 ms) is applied to CA3 axons every 20 s, and the recording and 417
stimulating electrodes are slowly advanced into the slice until the 418
maximal fEPSP amplitude is obtained. 419

After the baseline recording is stable for at least 10 min, a 420
stimulus–response curve is generated to analyze the efficacy of 421
basal synaptic transmission. Following progressively increasing 422
stimulation strengths, the synaptic responses rise until a PS 423
appears in the decaying phase of the fEPSP (a “supramaximal” 424
response). The experiment continues when this response satisfies 425
several criteria: (1) The amplitude of the supramaximal fEPSP 426
should not be less than 1.5 mV. (2) The amplitude of the presyn- 427
aptic fiber volley should be at least 2.5-fold less than the amplitude 428
of the fEPSPs. (3) The submaximal fEPSPs should not be 429
contaminated by other components. In Fig. 1, we show two 430
recording sites and the fEPSPs that were recorded at the *str. pyr.* 431
and *str. rad.* (Fig. 1a). 432

3.3. Induction of LTP In Vitro

LTP is a persistent increase in synaptic responses that is commonly 433
induced by HFS or TBS being applied to presynaptic fibers. For 434
LTP recordings, the following experimental design is used: 435

1. We recorded a stable baseline and determined the stimulation 436
intensity at which a supramaximal response is elicited (Fig. 1). 437
2. With a stimulation intensity generating fEPSPs with 50% of 438
the slope of the supramaximal fEPSPs, we recorded a baseline 439
every 20 s for at least 10 min. During the baseline recordings, 440
several aspects should be taken into consideration (see Notes, 441
Sect. 4). 442
3. After a stable baseline of the appropriate duration is recorded, 443
LTP is induced (Fig. 2). An efficient protocol is applying four 444
trains of TBS every 20 s. Each TBS consists of 8 bursts deliv- 445
ered at 5 Hz, and each burst consists of 4 pulses at 100 Hz. 446
However, different numbers of TBS and HFS episodes and 447
pharmacological manipulations are used to induce different 448
forms of LTP in various hippocampal synapses (Table 1). 449
These protocols share similar features with synaptic associative 450
memory mechanisms, such as rapid induction, synapse speci- 451
ficity, associative interactions, persistence, and a dependence 452
on correlated synaptic activity. 453
4. TBS induces a drastic potentiation of the fEPSP magnitude. 454
The initial phase of potentiation lasts about 2 min and is called 455
short-term potentiation (STP). It is followed by early LTP 456
(here called LTP for simplicity) that reaches its maximum 457
within about 10–20 min after TBS (Fig. 2b) and may persist 458
for several hours. To measure LTP, we use the average slope of 459
the fEPSPs that are recorded 50–60 min after TBS and express 460

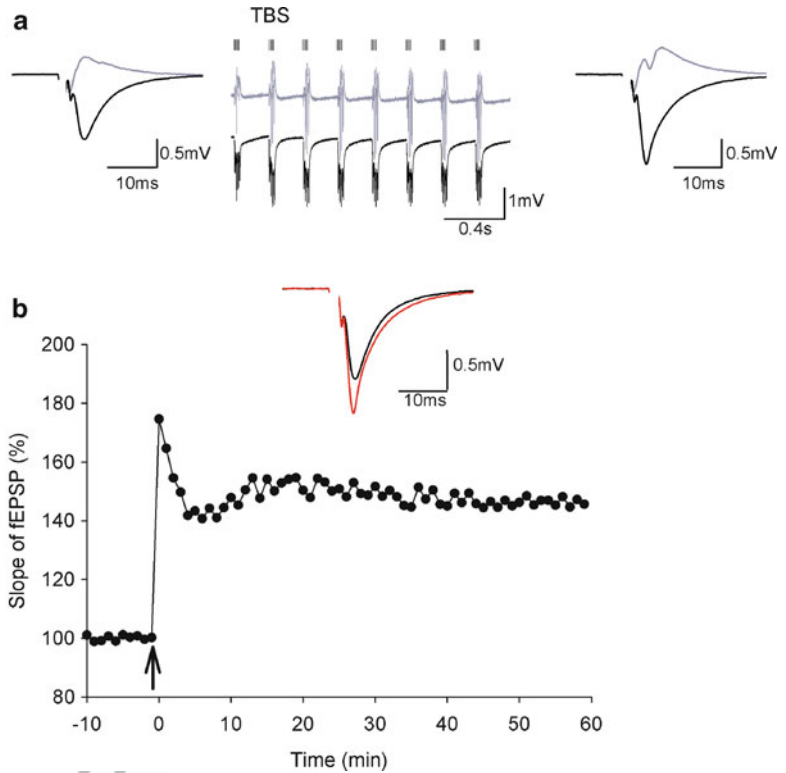


Fig. 2. LTP recordings in the CA3–CA1 connection in the hippocampus. (a) Representative traces of fEPSPs recorded in *stratum pyramidale* (gray) and *stratum radiatum* (black) are shown on the left panel). The average of 10 min of baseline (30 sweeps) is presented. Representative traces of TBS applied to induce LTP are shown in the middle panel). Four such TBSs were applied every 20 s. (Only the first TBS is presented in the graph). Recordings in the *stratum pyramidale* (upper gray) reveal the appearance of pop spikes during TBS, which were not detectable in the *stratum radiatum*. Recordings from the *stratum radiatum* during TBS reveal the facilitation of the fEPSPs. Responses averaging 50–60 min after LTP induction are presented in the right panel. The fEPSPs and PSs show significant increases; the appearance of the PS in the *stratum pyramidale* and an increase in the amplitude of the fEPSPs in the *stratum radiatum*. (b) A profile of TBS-induced LTP. (Upper) An overlay of the representative fEPSPs before (black trace) and after (red trace) the induction of LTP, as shown individually in panel (a). (Lower) Measurements of the slope of the fEPSP before, during and after LTP induction. Stimulation was delivered every 20 s. Significant STP (1–2 min) and LTP (50–60 min) of the fEPSPs was detected after TBS (indicated by arrow). The mean slope of the fEPSPs recorded 0–10 min before TBS is defined as 100%.

it as a percentage (where 10 min of baseline recording is 100%). It is important to control the amplitude of the presynaptic volleys (a small, short-lasting component that precedes the fEPSP) after LTP induction. This is a good measure of the number of stimulated axons, and its stability indicates that the same number of presynaptic fibers is recruited before and after LTP induction.

461
462
463
464
465
466
467

Table 1

The protocols used for the induction of LTP in different excitatory hippocampal synapses

Axonal projections	Postsynaptic area	Stimulation intensity	Pattern of stimulation	Pharmacology
PP	DG	100%	5×HFS	Picrotoxin
	CA1, CA3	100%	2×HFS	Picrotoxin
MF	CA3	Sufficient to elicit 40- to 60- μ V responses	2×HFS	AP5
CA3	CA1	50%	2×HFS	No
	CA3	50%	2×HFS	No

PP perforant path; MF mossy fibers; DG dentate gyrus; CA1, CA3 areas of the hippocampus (41)

3.4. Induction of LTP by HFS in Different Synaptic Pathways in the Hippocampus

As summarized in the Table 1 and Fig. 3, LTP can be reliably induced in seven major excitatory connections in hippocampal slices using several trains of HFS. Each train includes 100 pulses delivered at 100 Hz. The intertrain interval is 20 s, and the pulse duration is 0.1–0.2 ms.

1. To stimulate the associational/commissural projections and record the CA3–CA3 fEPSPs, one can place the stimulating electrode either in the *str. rad.* of the CA3 field and thus activate the associational fibers orthodromically, or one can place the electrode in the *str. rad.* of the CA1 field and activate the associational projections antidromically. We suggest using the latter approach to avoid the direct stimulation of the local CA3 interneurons. Because the CA3–CA3 synapses are located in the *str. rad.* of the CA3 field, the recording electrode is placed in this area. LTP is induced by two trains of HFS, with the stimulation intensity providing the fEPSPs with a magnitude of 50% of the supramaximal response.
2. To stimulate the Schaffer collateral/commissural projections and record the CA3–CA1 fEPSPs, the stimulating and recording electrodes are placed in the *str. rad.* of the CA1 region. For LTP induction, two trains of HFS are applied, with the stimulation intensity providing the fEPSPs with a magnitude of 50% of the supramaximal response (44, 45).
3. To record the direct perforant path-CA1 responses, we place the stimulating and recording electrodes in the *str. lac-mol.* of the CA1 field. The stimulating electrode is placed close to the subiculum. Because there is a high probability of activating the perforant path fibers that project to the DG (which may cause

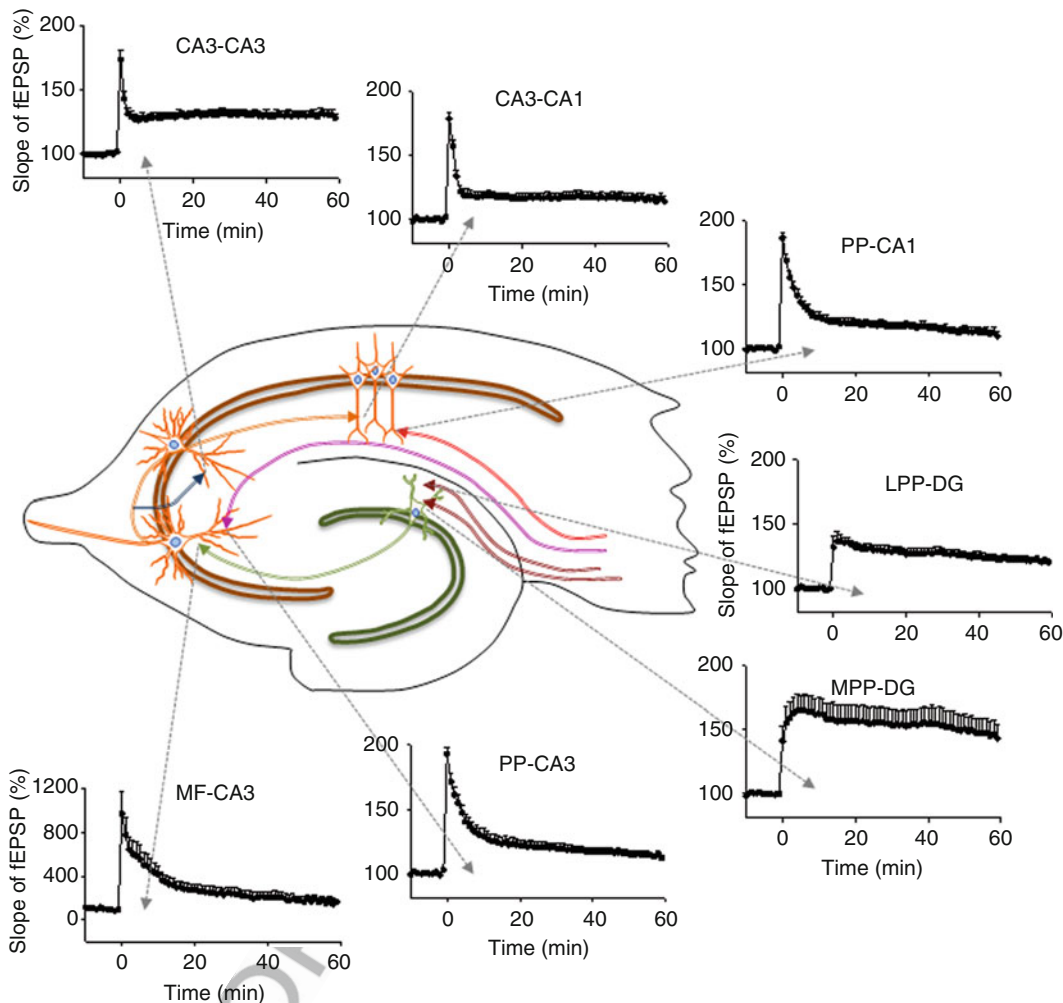


Fig. 3. A schematic illustration of the seven major excitatory synaptic connections and forms of LTP in the hippocampus. The synaptic connections from CA3 to CA3, from CA3 to CA1, from the dentate gyrus to CA3 and from the perforant path to all these regions are shown in a color-coded manner. The short- and long-term potentiation profiles are shown that were recorded in seven major excitatory synapses in the hippocampus of wild-type mice with a C57BL/6 background (for details, see ref. (41)). The data represent mean + SEM. The mean slope of the fEPSPs recorded 0–10 min before HFS is taken as 100%. For all recordings, the number of slices per LTP trace was on average 8 and the number of animals was 4. Reproduced with modifications and permission from ref. (41).

the polysynaptic activation of CA1 neurons), we cut the slices using a glass pipette through the DG and along the border between the CA1 and CA3 regions (46). LTP is induced by two trains of HFS delivered with a stimulation intensity that elicits supramaximal responses in disinhibited slices. For disinhibition, 100 μ M picrotoxin is applied to the slice 10 min before and during HFS.

4. To record the lateral perforant path (LPP)-dentate gyrus (DG) fEPSPs, the stimulating and recording electrodes are placed

496
497
498
499
500
501
502
503
504

- in the outer molecular layer of the DG. The responses are identified by the application of paired-pulse stimulation with 50-ms interstimulus intervals, and only the fEPSPs with paired-pulse facilitation are analyzed. LTP is induced by five trains of HFS using a supramaximal stimulation intensity in disinhibited slices (47). Disinhibition is required to induce LTP in mature perforant path synapses (48) and is achieved by the application of 100 μ M picrotoxin 10 min before and during HFS.
5. To record the medial perforant path (MPP)-DG fEPSPs, the stimulating and recording electrodes are placed in the inner molecular layer, and only the responses with paired-pulse depression are recorded further. LTP is induced as in the LPP-DG connections.
 6. To record the direct perforant path-CA3 responses, a stimulating electrode is placed in the *str. lac-mol.* of the CA1 field near the subiculum, and a recording electrode is placed in the *str. lac-mol.* of the CA3 field. To avoid the disynaptic activation of the CA3 pyramidal neurons, the slices are cut with a glass electrode through the DG (49). LTP is induced by two trains of HFS delivered with a supramaximal stimulation intensity. The slices are disinhibited with 100 μ M picrotoxin.
 7. To record the mossy fiber-CA3 fEPSPs, a stimulating electrode is placed in the DG near the internal side of granule cell layer, and a recording electrode is placed in the *stratum lucidum* (*str. luc.*) of the CA3 field. To avoid polysynaptic responses, a low stimulation intensity is used to elicit 40- to 60- μ V fEPSPs. The mossy fiber responses are identified by their short duration and a frequency-dependent facilitation of >200% that is elicited in response to a 0.33-Hz stimulation (50). Two trains of HFS are used for the induction of LTP (44). LTP at this synapse is known to be NMDA receptor-independent; therefore, 50 μ M AP5 is applied 15 min before and during HFS. To confirm that the recorded field EPSPs are evoked by the stimulation of the mossy fibers and are not contaminated by the associational/commissural pathway, a metabotropic glutamate receptor agonist (2 μ M DCGIV) is applied at the end of each experiment, and only the responses that are inhibited by >80% are assumed to be elicited by mossy fiber stimulation (51).

3.5. Induction of Oscillations by High-Frequency Stimulation

The recordings are performed in a submerged chamber at 30°C. Schaffer collateral commissural fibers are stimulated in the *str. rad.* with a bipolar tungsten stimulation electrode (WPI) or a glass pipette. After stable baseline recordings, the threshold of oscillation generation and their amplitude and duration are analyzed. Short trains of HFS are applied every 5 min with 50, 100, 150, 200, 250, 300, 350 and 400 μ A stimulation intensities. Short HFS contains

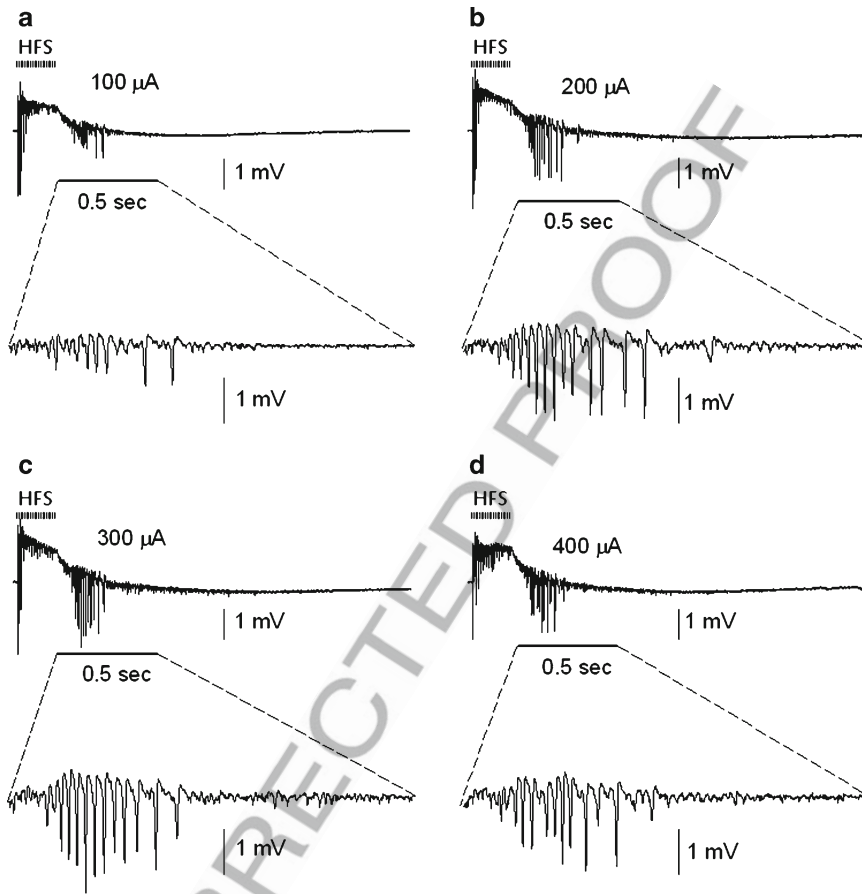


Fig. 4. HFS-induced high-frequency oscillations during neuronal activity. Representative traces of HFS-induced oscillatory activity recorded at the *stratum pyramidale* with different stimulation intensities (100, 200, 300, and 400 μA in **a**, **b**, **c**, and **d**, respectively). Each HFS contained 20 pulses at 100 Hz and was delivered in a 5-min interval. During HFS (*upper*), PSs are inhibited. Within about 0.2–0.3 s after HFS, induced oscillatory activity is generated. (Traces with a higher resolution after the subtraction of slow potentials are shown in the *lower panels*.) Oscillations are most prominent at stimulation intensities of 200–300 μA .

20 pulses that are applied at 100 Hz. The induced “ripple-like” oscillations are recorded within 2 s after the application of HFS. The induced oscillatory activity in the *str. pyr.* is detectable starting at 100 μA and is maximal at 200–300 μA (Fig. 4). To detect the induced oscillations, the traces are recorded for 2 s after the application of HFS. After the initial positive-going component, a slow negative-going component is detected in the *str. pyr.*, when spontaneous high-frequency oscillatory activity is generated.

3.6. Induction of LTP by a Protocol Eliciting High-Frequency Oscillations

The protocol used for the induction of oscillations results in an induction of LTP in the stimulated pathway (Fig. 5). During baseline recording, the stimulation intensity is set to elicit fEPSPs with 50% of the supramaximal intensity. During an HFS of 20 pulses at 100 Hz, the stimulation intensity is fivefold

551
552
553
554
555
556
557
558
559
560
561
562
563

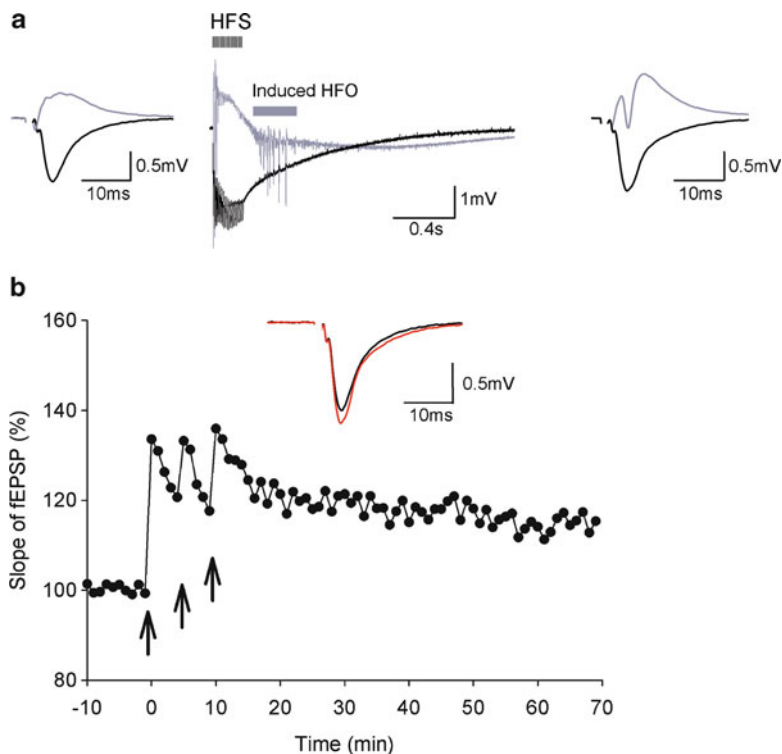


Fig. 5. HFS-induced oscillations and associated LTP. (a) Representative fEPSPs before (left) and after the induction of LTP (right), which were recorded in the *stratum pyramidale* (gray) and the *stratum radiatum* (black), are presented as in Fig. 2. To induce LTP, three trains of HFS were applied with 5-min intervals. Each HFS contained 20 pulses at 100 Hz. Baseline responses were monitored every 20 s. The stimulation intensity during HFS was set to be five times higher than during baseline recording. The HFS applied at this stimulation strength induced oscillatory activity. (b) A profile of HFS-induced LTP. (Upper panel) Superimposed representative fEPSPs before (black trace) and after the induction (red trace) of LTP that were shown individually in (a). (Lower panel) Measurement of fEPSP slopes before and after LTP induction. Three trains of HFS were delivered every 5 min (indicated by arrows). Significant STP (1–2 min) and LTP (50–60 min) of the fEPSPs is detected after TBS. The mean slope of the fEPSPs recorded 0–10 min before TBS is defined as 100%.

higher than during baseline recording (because such a stimulation intensity is the most effective for inducing oscillations). After HFS, the stimulation intensity is reset to the intensity that has been used for the baseline recordings. To induce LTP, three trains of HFS are delivered at 5-min intervals. The recording of fEPSPs for 1 h reveals that robust LTP can be induced by this protocol (Fig. 5).

564
565
566
567
568
569
570

4. Notes

571

4.1. Mice for LTP Recordings

LTP can be easily induced in slices derived from mice of different ages. However, the age should be within a well-defined interval, because some forms of LTP exhibit age-dependence, and there can be a gene-dependent interaction between age and synaptic plasticity in genetically modified mice (44). Two ages are particularly attractive: 3 weeks (if the extracellular recordings will be complemented with a patch-clamp study) and 3 months (if the electrophysiological recordings will be complemented by a behavioral analysis of cognitive function). The level of LTP significantly depends on the genetic background of the mouse strain that is used in the experiments. Therefore, the use of wild-type littermate controls is highly recommended, particularly if the background of the genetically modified mice is mixed or the mice were not inbred for more than six generations. If the mice originate from different parents, it is important that they are raised under identical conditions. If the animal facility is located in a building that is different from where the experiments are performed, the mice should be brought into the laboratory at 1 day before the start of experiment and kept in a quiet place to minimize the possible effect of stress on synaptic plasticity. Acute or chronic stresses can easily alter LTP, and therefore, investigators should minimize their effects as much as possible before slice preparation.

572
573
574
575
576
577
578
579
580
581
582
583
584
585
586
587
588
589
590
591
592
593

4.2. Brain Slicing

The blade should be cleaned in acetone for several minutes and then washed in water. The blade should be fixed securely and adjusted in the blade holder to ensure that the blade is parallel to the brain tissue. The age of the animals plays an important role in determining the thickness of the slices being prepared. We used 350- μ m-thick hippocampal slices for 2- to 3-month-old mice. For animals younger than 1 month, 400 μ m-thick slices are used. For animals older than 3 months (up to 24 months), 300- μ m-thick slices are used.

594
595
596
597
598
599
600
601

4.3. Construction and Use of the Incubation Chamber

A chamber for the incubation of brain slices can be made from a plastic vessel (10 cm in diameter and height), inside which a plastic cylinder (5 cm in diameter, 3 cm in height) is glued in the middle of the wall. The slices are placed at the bottom of the cylinder, which can be made of nylon stockings glued to the edges of the cylinder. The vessel is filled with ACSF to the top of the cylinder. The diffuser (connected to oxygenation tubing) is placed at the bottom of the vessel (outside of cylinder), and the gas pressure is adjusted to saturate the solution but avoid any movement of the floating slices. At the end of each slice preparation, all of the instruments and the vibratome should be washed and dried to avoid agar soiling.

602
603
604
605
606
607
608
609
610
611
612
613

4.4. Slice Handling in the Recording Chamber

The slice is placed on the recording platform and covered with a nylon mesh. The mesh is placed on top of slice such that a hole cut in the mesh is located above the hippocampus. The mesh is fixed with two small metal loads to prevent the slice from floating. The recording chamber is continuously perfused (3 ml/min) with freshly prepared ACSF via a tubing system that connects a reservoir containing ACSF to the recording chamber (using the force of gravity). In such a configuration, a hippocampus is supplied with ACSF from both sides, which is believed to be more efficient for keeping the hippocampal slice viable during long-lasting recordings than the traditional method, in which ACSF is mostly supplied from the top. Before entering the recording chamber, the ACSF is warmed by a mounted-line heater, which keeps the fluid at a constant 30°C temperature. (Even a slight fluctuation in temperature can significantly affect the fEPSP.) The ACSF is drawn from the recording chamber with the peristaltic pump in a timely manner and delivered back into plastic reservoir, thereby achieving circulated perfusion. The ACSF is oxygenated with 95% O₂ and 5% CO₂ for at least for 30 min prior to all of the recordings and continuously during all of the recordings.

4.5. Mastering Baseline Recording

The stability of baseline fEPSPs is “the must” for LTP recording and its subsequent analysis. There should be no tendency for fEPSPs to run up or down. Otherwise, one should wait until the fEPSP responses have stabilized and then remeasure the stimulus–response curve. For the stability of the fEPSP recordings, it is important to have a constant ACSF flow rate, oxygenation and temperature during the recording of one slice and for different slices and animals. The time for the baseline recordings depends on the time-course of the LTP recordings. If early LTP is not studied for more than 1 h, it is sufficient to record the baseline for 10–20 min. In case of late LTP recordings (recordings for 4–8 h after the induction of LTP), a stable baseline should be monitored for 30 min to 1 h.

Acknowledgments

This work was supported by Italian Institute of Technology and by grants from the Deutsche Forschungsgemeinschaft (DI 702/6-1 to A.D.) and the San Paolo “Programma in Neuroscienze” (to A.D.).

652 References

- 654 1. Bliss TV, Lomo T (1973) Long-lasting potentiation of synaptic transmission in the dentate
655 area of the anaesthetized rabbit following
656 stimulation of the perforant path. *J Physiol*
657 232(2):331–356
658
- 659 2. Lynch MA (2004) Long-term potentiation
660 and memory. *Physiol Rev* 84(1):87–136
- 661 3. Andersen P, Morris R, Amaral D et al (2007)
662 The hippocampus book. Oxford University
663 Press, New York
- 664 4. Chapman PF, Kairiss EW, Keenan CL et al
665 (1990) Long-term synaptic potentiation in
666 the amygdala. *Synapse* 6(3):271–278
- 667 5. Rogan MT, Stäubli UV, LeDoux JE (1997)
668 Fear conditioning induces associative long-
669 term potentiation in the amygdala. *Nature*
670 390(6660):604–607
- 671 6. Dityatev AE, Bolshakov VY (2005) Amygdala,
672 long-term potentiation, and fear condition-
673 ing. *Neuroscientist* 11(1):75–88
- 674 7. Crepel F, Jaillard D (1991) Pairing of pre- and
675 postsynaptic activities in cerebellar Purkinje
676 cells induces long-term changes in synaptic
677 efficacy *in vitro*. *J Physiol* 432:123–141
- 678 8. Jörntell H, Hansel C (2006) Synaptic
679 memories upside down: bidirectional plasticity
680 at cerebellar parallel fiber-Purkinje cell
681 synapses. *Neuron* 52(2):227–238
- 682 9. Laroche S, Jay TM, Thierry AM (1990) Long-
683 term potentiation in the prefrontal cortex fol-
684 lowing stimulation of the hippocampal CA1/
685 subicular region. *Neurosci Lett* 114
686 (2):184–190
- 687 10. Alonso A, de Curtis M, Llinás R (1990) Post-
688 synaptic Hebbian and non-Hebbian long-
689 term potentiation of synaptic efficacy in the
690 entorhinal cortex in slices and in the isolated
691 adult guinea pig brain. *Proc Natl Acad Sci U S*
692 *A* 87(23):9280–9284
- 693 11. Artola A, Singer W (1987) Long-term poten-
694 tiation and NMDA receptors in rat visual cor-
695 tex. *Nature* 330(6149):649–652
- 696 12. Iriki A, Pavlides C, Keller A et al (1989) Long-
697 term potentiation in the motor cortex. *Science*
698 245(4924):1385–1387
- 699 13. Uhlhaas PJ, Singer W (2010) Abnormal
700 neural oscillations and synchrony in schizo-
701 phrenia. *Nat Rev Neurosci* 11(2):100–113
- 702 14. Engel AK, Moll CK, Fried I et al (2005) Inva-
703 sive recordings from the human brain: clinical
704 insights and beyond. *Nat Rev Neurosci* 6
705 (1):35–47
- 706 15. Buzsáki G (2006) Rhythms in the brain.
707 Oxford University Press, New York
16. Buzsáki G (2002) Theta oscillations in the
708 hippocampus. *Neuron* 33(3):325–340
709
17. Buzsáki G (2004) Large-scale recording of neu-
710 ronal ensembles. *Nat Neurosci* 7(5):446–451
711
18. Lisman J, Buzsáki G (2008) A neural coding
712 scheme formed by the combined function of
713 gamma and theta oscillations. *Schizophr Bull*
714 34(5):974–980
715
19. Buzsáki G, Eidelberg E (1983) Phase relations
716 of hippocampal projection cells and interneu-
717 rons to theta activity in the anesthetized rat.
718 *Brain Res* 266(2):334–339
719
20. O'Keefe J (1993) Hippocampus, theta, and
720 spatial memory. *Curr Opin Neurobiol* 3
721 (6):917–924
722
21. Moser EI, Kropff E, Moser MB (2008) Place
723 cells, grid cells, and the brain's spatial repre-
724 sentation system. *Annu Rev Neurosci*
725 31:69–89
726
22. Winson J (1978) Loss of hippocampal theta
727 rhythm results in spatial memory deficit in the
728 rat. *Science* 201(4351):160–163
729
23. Bikbaev A, Manahan-Vaughan D (2007) Hip-
730 pocampal network activity is transiently altered
731 by induction of long-term potentiation in the
732 dentate gyrus of freely behaving rats. *Front*
733 *Behav Neurosci* 1:7
734
24. Bikbaev A, Manahan-Vaughan D (2008) Rela-
735 tionship of hippocampal theta and gamma
736 oscillations to potentiation of synaptic trans-
737 mission. *Front Neurosci* 2(1):56–63
738
25. Hyman JM, Wyble BP, Goyal V et al (2003)
739 Stimulation in hippocampal region CA1 in
740 behaving rats yields long-term potentiation
741 when delivered to the peak of theta and long-
742 term depression when delivered to the trough.
743 *J Neurosci* 23(37):11725–11731
744
26. Hölscher C, Anwyl R, Rowan MJ (1997)
745 Stimulation on the positive phase of hippo-
746 campal theta rhythm induces long-term
747 potentiation that can be depotentiated by
748 stimulation on the negative phase in area
749 CA1 *in vivo*. *J Neurosci* 17(16):6470–6473
750
27. Pavlides C, Greenstein YJ, Grudman M
751 (1988) Long-term potentiation in the dentate
752 gyrus is induced preferentially on the positive
753 phase of theta-rhythm. *Brain Res* 439
754 (1–2):383–387
755
28. Greenstein YJ, Pavlides C, Winson J (1988)
756 Long-term potentiation in the dentate gyrus is
757 preferentially induced at theta rhythm period-
758 icity. *Brain Res* 438(1–2):331–334
759
29. Orr G, Rao G, Houston FP et al (2001)
760 Hippocampal synaptic plasticity is modulated
761

- 762 by theta rhythm in the fascia dentata of adult
763 and aged freely behaving rats. *Hippocampus*
764 11(6):647–654
- 765 30. Poe GR, Nitz DA, McNaughton BL et al
766 (2000) Experience-dependent phase-reversal
767 of hippocampal neuron firing during REM
768 sleep. *Brain Res* 855(1):176–180
- 769 31. Huerta PT, Lisman JE (1995) Bidirectional
770 synaptic plasticity induced by a single burst
771 during cholinergic theta oscillation in CA1
772 in vitro. *Neuron* 15(5):1053–1063
- 773 32. Huerta PT, Lisman JE (1993) Heightened
774 synaptic plasticity of hippocampal CA1 neu-
775 rons during a cholinergically induced rhythmic
776 state. *Nature* 364(6439):723–725
- 777 33. Hájos N, Pálhalmi J, Mann EO et al (2004)
778 Spike timing of distinct types of GABAergic
779 interneuron during hippocampal gamma oscill-
780 ations in vitro. *J Neurosci* 24(41):9127–9137
- 781 34. Csicsvari J, Jamieson B, Wise KD et al (2003)
782 Mechanisms of gamma oscillations in the hip-
783 pocampus of the behaving rat. *Neuron* 37
784 (2):311–322
- 785 35. Traub RD, Whittington MA, Colling SB et al
786 (1996) Analysis of gamma rhythms in the rat
787 hippocampus in vitro and in vivo. *J Physiol*
788 493(Pt 2):471–484
- 789 36. Pöschel B, Heinemann U, Draguhn A (2003)
790 High frequency oscillations in the dentate
791 gyrus of rat hippocampal slices induced by
792 tetanic stimulation. *Brain Res* 959
793 (2):320–327
- 794 37. Goutagny R, Jackson J, Williams S (2009)
795 Self-generated theta oscillations in the hip-
796 pocampus. *Nat Neurosci* 12(12):1491–1493
- 797 38. Singer W, Gray CM (1995) Visual feature inte-
798 gration and the temporal correlation hypothe-
799 sis. *Annu Rev Neurosci* 18:555–586
- 800 39. Colgin LL, Denninger T, Fyhn M et al (2009)
801 Frequency of gamma oscillations routes flow
802 of information in the hippocampus. *Nature*
803 462(7271):353–357
- 804 40. Wespátat V, Tennigkeit F, Singer W (2004)
805 Phase sensitivity of synaptic modifications in
806 oscillating cells of rat visual cortex. *J Neurosci*
807 24(41):9067–9075
- 808 41. Morellini F, Lepsveridze E, Kähler B et al
809 (2007) Reduced reactivity to novelty, impaired
810 social behavior, and enhanced basal synaptic
811 excitatory activity in perforant path projec-
812 tions to the dentate gyrus in young adult
813 mice deficient in the neural cell adhesion mol-
ecule CHL1. *Mol Cell Neurosci* 34
(2):121–136
- 814 42. Kochlamazashvili G, Senkov O, Grebenyuk S
815 et al (2010) Neural adhesion molecule-
816 associated polysialic acid regulates synaptic
817 plasticity and learning by restraining the sig-
818 naling through GluN2B-containing NMDA
819 receptors. *J Neurosci* 30(11):4171–4183
- 820 43. Claiborne BJ, Xiang Z, Brown TH (1993)
821 Hippocampal circuitry complicates analysis of
822 long-term potentiation in mossy fiber
823 synapses. *Hippocampus* 3(2):115–121
- 824 44. Eckhardt M, Bukalo O, Chazal G et al (2000)
825 Mice deficient in the polysialyltransferase
826 ST8SiaIV/PST-1 allow discrimination of
827 the roles of neural cell adhesion molecule pro-
828 tein and polysialic acid in neural development
829 and synaptic plasticity. *J Neurosci* 20
830 (14):5234–5244
- 831 45. Muller D, Wang C, Skibo G et al (1996) PSA-
832 NCAM is required for activity-induced synap-
833 tic plasticity. *Neuron* 17(3):413–422
- 834 46. Remondes M, Schuman EM (2003) Molecu-
835 lar mechanisms contributing to long-lasting
836 synaptic plasticity at the temporoammonic-
837 CA1 synapse. *Learn Mem* 10(4):247–252
- 838 47. Evers MR, Salmen B, Bukalo O et al (2002)
839 Impairment of L-type Ca²⁺ channel-depen-
840 dent forms of hippocampal synaptic plasticity
841 in mice deficient in the extracellular matrix
842 glycoprotein tenascin-C. *J Neurosci* 22
843 (16):7177–7194
- 844 48. Hanse E, Gustafsson B (1992) Long-term
845 potentiation and field EPSPs in the lateral
846 and medial perforant paths in the dentate
847 gyrus in vitro: a comparison. *Eur J Neurosci*
848 4(11):1191–1201
- 849 49. Berzhanskaya J, Urban NN, Barrionuevo G
850 (1998) Electrophysiological and pharmaco-
851 logical characterization of the direct perforant
852 path input to hippocampal area CA3. *J Neu-
853 rophysiol* 79(4):2111–2118
- 854 50. Bukalo O, Fentrop N, Lee AY et al (2004)
855 Conditional ablation of the neural cell adhe-
856 sion molecule reduces precision of spatial
857 learning, long-term potentiation, and depres-
858 sion in the CA1 subfield of mouse hippocam-
859 pus. *J Neurosci* 24(7):1565–1577
- 860 51. Cremer H, Chazal G, Carleton A et al (1998)
861 Long-term but not short-term plasticity at
862 mossy fiber synapses is impaired in neural cell
863 adhesion molecule-deficient mice. *Proc Natl
864 Acad Sci U S A* 95(22):13242–13247